Ouput-Feedback Control of Combined Sewer Networks through Receding Horizon Control with Moving Horizon Estimation

Bernat Joseph-Duran[b], Carlos Ocampo-Martinez[a], Gabriela Cembrano[a,b]

[a] Institut de Robòtica i Informàtica Industrial (CSIC-UPC),
Universitat Politècnica de Catalunya, Barcelona, Spain.
[b] CETAQUA Water Technology Center (Agbar-CSIC-UPC), Barcelona, Spain.

Abstract

An output-feedback control strategy for pollution mitigation in combined sewer networks is presented. The proposed strategy provides means to apply model-based predictive control to large-scale sewer networks, in-spite of the lack of measurements at most of the network sewers. In previous works, the authors presented a hybrid linear control-oriented model for sewer networks together with the formulation of Optimal Control Problems (OCP) and State Estimation Problems (SEP). By iteratively solving these problems, preliminary Receding Horizon Control with Moving Horizon Estimation (RHC/MHE) results, based on flow measurements, were also obtained. In this work, the RHC/MHE algorithm has been extended to take into account both flow and water level measurements and the resulting control loop has been extensively simulated to assess the system performance according different measurement availability scenarios and rain events. All simulations have been carried out using a detailed physically-based model of a real case-study network as virtual reality.

1 Introduction

Public sewer networks can be classified into separate sewer networks and combined sewer networks. In separate sewer networks, both wastewater (domestic, commercial and industrial) and stormwater are conveyed to treatment facilities through two separate pipe systems, while in combined sewer networks a single pipe system for both types of water exists. During heavy rain events the volumetric capacity of combined sewer networks can be overloaded leading to untreated water discharges to surrounding water bodies known as Combined Sewer Overflows (CSOs). To reduce the frequency and intensity of CSOs, combined sewer networks are equipped with flow regulation and storage elements that can be operated by means of different control strategies: from fully automatic control to passive control or even expert operator man-made decisions.

During the last two decades a number of automatic control strategies for flow regulation in combined sewer networks to mitigate CSO events and reduce pollution in the surrounding water bodies have appeared in the literature [15, 35, 6, 24, 29, 26, 27, 39, 19]. Among these strategies, Real-Time Control (RTC) is widely regarded as the best option [37], since it is based on recomputing the control actions every few minutes by using the last available network measurements and rainfall forecasts. On the other hand, RTC strategies cannot rely on algorithms requiring extensive computation, since in that case the up-to-date information from sensors and forecasts would be obsolete by the time the computations were finished, ruining the main feature of the technique.

The classical physically-based model obtained by applying the principles of mass and energy conservation to water transport in open channels is based on a set of partial differential equations (the de Saint-Venant equations [7]). The numerical solution of these equations can only be obtained by means of algorithms of high computational burden. Therefore, these algorithms cannot be included in the computation of control actions in an RTC strategy for most sewer networks [37, 32]. To overcome this problem, it is a common practice that RTC strategies are based on simplified models of the network dynamics (that is, the temporal evolution of flows and volumes along the network). Simplified models can be obtained in a number of ways: manipulation of the physically-based equations (omission of some phenomena, linearization, discretization), conceptual models (mathematical description of the most relevant properties

of the system) or identification-based models (obtained from data) (see [18] for examples of each type of model for flow-routing applications).

In a RTC strategy, the simplified model, called the control model, is used to predict the future state of the system over a finite time window according to different control actions (mostly gate, pump or weir flows) and rainfall forecasts. These predictions are systematically evaluated to come up with the most convenient control actions by means of an Optimal Control Problem (OCP). This procedure is repeated every few minutes taking into account new rainfall forecasts, updating the model initial conditions using the last available measurements and moving the prediction time window in a so-called Receding Horizon Control strategy (RHC; also known as Model Predictive Control, MPC) [3, 33].

A drawback of the model-predictive RHC technique for combined sewer networks is the need for full-state initial conditions to update the model at each computation. Combined sewer networks are usually large-scale systems for which only a limited number of measurement points are available. Therefore, to apply the RHC strategy, state estimation techniques must be included in the closed-loop control scheme. However, since RTC techniques are usually tested against detailed model simulators providing all the system variables, measurement availability and state estimation techniques are often not considered.

In a previous work [22], a hybrid linear delayed control model for combined sewer networks was introduced, together with calibration procedures, validation results and sensitivity analysis for a real case study. Preliminary RHC results were also provided, assessing the performance of a model-based controller in minimizing CSOs and urban flooding during heavy rain events and proving to provide a notable improvement with respect to a passive control approach. Since the proposed model is based only on flows and volumes, the presented controller acts as an upper layer controller, computing set-points for the local controllers located at the network gates, which adjust the gate positions accordingly. Closed-loop simulations were performed using a detailed physically-based model simulator of the case study network as virtual reality. The physically-based model simulator provided not only a realistic way to assess the closed-loop controller performance but also a means to obtain on-line measurements of the network status. However, in that first step, closed-loop simulations were carried out under the assumption of full-state measurement availability of flows at all the network sewers. This is, indeed, an unrealistic assumption, since due to the large-scale nature of sewer networks, measurements are only available at some particular points. Moreover, in combined sewer networks, the measurements can take the form of both flow and water level measurements, with the latter being the most common ones due to precision, maintenance and economic reasons [5].

The main objective of this work is to extend the RHC approach outlined in [22] to take into account the available number and type (flow or water level) of measurements and to assess the performance of the system according to different measurement availability scenarios. To this end, a model-based State Estimation Problem (SEP) is presented to be used to reconstruct the whole combined sewer system state out of a few measurements. As in the RHC strategy, the SEP problem is solved at each control iteration based on the last available measurements and moving the estimation time window in a so-called Moving Horizon Estimation (MHE) strategy. The state estimate resulting of each SEP is used to update the initial conditions of a model-based OCP according to the RHC technique. Since the model in [22] is a hybrid linear model, both the SEP and the OCP result in constrained Mixed Integer Linear Programming (MILP) problems. The proposed closed-loop RHC/MHE algorithm is then tested using a commercial physically-based model simulator as virtual reality and considering different configurations for the measurement availability, including flow measurements and water level measurements. The results of these simulations are used to assess which is the best measurement configuration by comparing the results against the full-state measurement case.

The choice of the estimation technique is based on the properties of the process and control models. As mentioned above, in the process model used for closed-loop simulations water motion is described by a set of partial differential equations, which prevents the use of nonlinear estimation and error-based output-feedback techniques, as well as the application of theoretical results (convergence, closed-loop stability, etc.), for discrete-time systems or differential equation systems [25, 33, 30, 31]. Furthermore, since the control model is based on a constrained hybrid system, usual estimation techniques such as the Luenberger observer or the (extended) Kalman filter do not apply. The proposed SEPs consists in a 1-norm variation of the deadbeat observer proposed in [2], which is suitable for hybrid systems. Although the observability and convergence tests for this type of systems discussed in [1, 14] cannot be applied, since they rely on the assumption that the process model is also a hybrid linear model, simulation results for number of different rain events and measurement availability scenarios show the accuracy and suitability of the proposed approach.

The remainder of the paper is organized as follows: in Section 2 an outline of the model described in [22] is provided together with its general mathematical expression, the formulation of the OCP and SEP and the description of the RHC/MHE algorithm. Section 3 provides a brief description of the case study sewer network and a discussion of the closed-loop simulation results and computational details of the RHC/MHE strategy for several real rain events taking into account the following measurement scenarios: full flow measurements, limited flow measurements, limited water level measurements and mixed flow and water-level measurements. Finally, in Section 4, conclusions of the whole work are given together with some future research lines.

2 Combined Sewer Network Modeling, Control and Estimation

2.1 Sewer Network Model

The control and estimation techniques developed in this paper are based on the hydraulic hybrid linear model for sewer networks presented in [22]. The model describes volumes stored in detention tanks, flows through sewers, collectors (big sewers with storage capacity, modeled by using a tanks-in-series model that takes into account inflow delay and storage capacity) and weirs, overflows and flood runoff reentering the network after an overflow event. The basic flow equations take into account transport delay and flow attenuation along sewers and mass balance in junctions.Rain inflows to the network appear in the control model as forecasted disturbances with known values. They are obtained by means of a separate hydrologic rainfall-runoff model, which computes net inflows to the network from rain intensity data [11].

To keep the model useful for practical real-time applications in large-scale networks, modeling of backwater effects by means of water level variables and flow-level relations is not included in the model. Such a modeling approach would turn the OCPs and SEPs into *mixed integer nonlinear problems* (MINLP) of very high computational burden in the case of large-scale systems. Therefore, this approach (although without integer variables) has only been applied to small network instances [36, 9, 13] or to irrigation channels with simple topologies [40, 34].

Equations for weirs, overflows and flood runoff contain maximum and minimum functions that make the model nonlinear. These elements have been modeled by using piecewise linear equations, and have been reformulated by means of the Mixed Logical Dynamic (MLD) systems approach to obtain a set of linear equations and inequalities involving binary variables [3]. After the MLD reformulation is performed, the complete sewer network model can be written in the following form:

$$\begin{aligned} \sum_{i=0}^{T} M_i X(t-i) &= m(t), \\ \sum_{i=0}^{T} N_i X(t-i) &\leq n(t), \end{aligned} \tag{1}$$

where $X(t)$ contains all the system variables at the discrete-time instant t, including states, inputs, outputs and binary variables arising from the MLD reformulation. Matrices M_i and N_i, $i = 1, \ldots, T$, where T is the maximum system delay, contain the coefficients of the system equations and MLD inequalities computed using the network topology description and the element parameters [22, 18]. Finally, vectors $m(t)$ and $n(t)$ contain the influence of both rain inflows and constants introduced in the MLD reformulation.

In [22], in addition to a complete description of the model and parameter calibration procedures, validation results and sensitivity analysis for the case study described in Section 3.1 are provided.

2.2 Optimal Control Problem Formulation

To formulate the OCP associated to the control oriented model (1), first the model is extended to include the network equations and MDL inequalities at several time instants ahead in the future as follows:

$$\begin{aligned} \sum_{i=0}^{T} M_i X(t-i+k) &= m(t+k), \quad k = 1, \ldots, H, \\ \sum_{i=0}^{T} N_i X(t-i+k) &\leq n(t+k), \quad k = 1, \ldots, H, \end{aligned} \tag{2}$$

where H is called the *prediction horizon* [3, 33].

At time instant t, it is assumed that all the network variables at the current and $T-1$ previous time instants are known, either through direct measurement or by means of an estimation procedure, as detailed in the next section. These measured or estimated variables, denoted $\hat{X}(t)$, are collected together in the vector of initial conditions

$$\mathcal{X}_0(t) = (\hat{X}(t)^\top, \ldots, \hat{X}(t-T+1)^\top)^\top. \tag{3}$$

Forecasts of the rain inflows to the network are also assumed to be available to compute the independent terms $m(t+k)$ and $n(t+k)$, $k = 1, \ldots, H$. Finally, to express the OCP in a compact matrix form, also the following vector collecting all the system variables at H future time steps is defined:

$$\mathcal{X}(t) = (X(t+H)^\top, \ldots, X(t+1)^\top)^\top, \tag{4}$$

and the following block matrices:

$$\mathcal{M}_1 = \begin{pmatrix} M_0 & M_1 & \ldots & \ldots & M_T & & \\ & \ddots & & & & \ddots & \\ & & M_0 & M_1 & \ldots & \ldots & M_T \\ & & & M_0 & \ldots & \ldots & M_{T-1} \\ & & & & \ddots & & \vdots \\ & & & & & M_0 & M_1 \\ & & & & & & M_0 \end{pmatrix} \Bigg\} \begin{matrix} H \\ \text{blocks} \end{matrix}, \quad \mathcal{M}_2 = - \begin{pmatrix} & & & & & & \\ & & & & & & \\ & & & & & & \\ M_T & & & & & & \\ M_{T-1} & M_T & & & & & \\ \vdots & \vdots & \ddots & & & & \\ M_2 & M_3 & \ldots & M_T & & & \\ M_1 & M_2 & \ldots & M_{T-1} & M_T & & \end{pmatrix} \Bigg\} \begin{matrix} H \\ \text{blocks} \end{matrix}, \tag{5}$$

$$\mathcal{M}_3(t) = (m(t+H)^\top, \ldots, m(t+1)^\top)^\top, \tag{6}$$

with analogous expressions for $\mathcal{N}_1$, $\mathcal{N}_2$ and $\mathcal{N}_3$. For the construction of these matrices it has been assumed that $H > T$, that is, the prediction horizon is greater than the largest delay in the system. Although this is not a necessary condition for the formulation of the OCP, it is a common assumption that allows the OCP to evaluate the performance of the system taking into account all the effects of the network dynamics.

Now, the OCP can be stated as

$$\begin{aligned} OCP(t): \qquad & \min_{\mathcal{X}(t)} \; J(\mathcal{X}(t)) = c^\top \mathcal{X}(t), \\ & \text{s.t.} \quad \mathcal{M}_1 \mathcal{X}(t) = \mathcal{M}_2 \mathcal{X}_0(t) + \mathcal{M}_3(t), \\ & \qquad \mathcal{N}_1 \mathcal{X}(t) \leq \mathcal{N}_2 \mathcal{X}_0(t) + \mathcal{N}_3(t), \\ & \qquad A_{eq} \mathcal{X}(t) = b_{eq}(t), \\ & \qquad A_{ineq} \mathcal{X}(t) \leq b_{ineq}(t). \end{aligned} \tag{7}$$

Details on the form of the cost function $J(\mathcal{X}(t))$ used to quantify common management objectives for sewer network control are given in Section 3.1. Since $J(\mathcal{X}(t))$ is a linear function and some of the variables involved in vector $\mathcal{X}(t)$ are binary, the OCP is an MILP problem.

Additional constraints of the form $A_{eq}\,\mathcal{X}(t) = b_{eq}(t)$ and $A_{ineq}\,\mathcal{X}(t) \leq b_{ineq}(t)$, are added to the OCP to take into account bounds on variables, bounds on the variation of the gate flows for smooth control actions and some additional mass balances not included in the basic model equations.

See [20, 18] for additional details.

2.3 State Estimation Problem Formulation

The SEP formulation [23] is analogous to the OCP one, but in this case the system dynamics and inequality constraints are enforced for the past states rather than for the future ones, as described in Equation 8.

$$\begin{aligned} & \sum_{i=0}^{T} M_i X_{\mathcal{O}}(t-i+k) = m(t+k), \\ & \sum_{i=0}^{T} N_i X_{\mathcal{O}}(t-i+k) \leq n(t+k), \\ & \qquad k = -H_{\mathcal{O}} + T + 1, \ldots, 0, \end{aligned} \tag{8}$$

where $H_{\mathcal{O}}$ is the number of past instant measured variables that will be used in the problem formulation. The vector of unknown variables for the SEP is then defined as

$$\mathcal{X}_{\mathcal{O}}(t) = (X_{\mathcal{O}}(t)^\top, \ldots, X_{\mathcal{O}}(t - H_{\mathcal{O}} + 1)^\top)^\top. \tag{9}$$

Vectors $X_{\mathcal{O}}(t)$ are defined in the same way as $X(t)$, but a different notation is used to distinguish the variables of the SEP and OCP in the closed-loop algorithm.

To express the constraints in matrix form, the following matrices are defined:

$$\mathcal{M}_1^{\mathcal{O}} = \left(\begin{array}{ccccccc} M_0 & M_1 & \ldots & M_{T-1} & M_T & & \\ & \ddots & \ddots & & \ddots & \ddots & \\ & & M_0 & M_1 & \ldots & M_{T-1} & M_T \end{array} \right) \Bigg\} \begin{array}{l} H_{\mathcal{O}} - T \\ \text{blocks,} \end{array} \tag{10}$$

$$\mathcal{M}_2^{\mathcal{O}}(t) = (m_{\mathcal{O}}(t)^\top, \ldots, m_{\mathcal{O}}(t - H_{\mathcal{O}} + 1)^\top)^\top, \tag{11}$$

with analogous expressions for $\mathcal{N}_1^{\mathcal{O}}$ and $\mathcal{N}_2^{\mathcal{O}}$.

Now, the state estimation problem can be written as

$$\begin{aligned} SEP(t): \quad & \min_{\{X_{\mathcal{O}}(t),\, \varepsilon_{\mathcal{Y}},\, \varepsilon_{\mathcal{U}}\}} \ \mathbf{1}_{\mathcal{Y}}^\top \varepsilon_{\mathcal{Y}} + \mathbf{1}_{\mathcal{U}}^\top \varepsilon_{\mathcal{U}}, \\ & \text{s.t.} \quad \mathcal{M}_1^{\mathcal{O}}\, \mathcal{X}_{\mathcal{O}}(t) = \mathcal{M}_2^{\mathcal{O}}(t), \\ & \qquad \mathcal{N}_1^{\mathcal{O}}\, \mathcal{X}_{\mathcal{O}}(t) \leq \mathcal{N}_2^{\mathcal{O}}(t), \\ & -\varepsilon_{\mathcal{Y}} \leq \Pi_{\mathcal{Y}}\, \mathcal{X}_{\mathcal{O}}(t) - \hat{\mathcal{Y}}(t) \leq \varepsilon_{\mathcal{Y}}, \\ & -\varepsilon_{\mathcal{U}} \leq \Pi_{\mathcal{U}}\, \mathcal{X}_{\mathcal{O}}(t) - \hat{\mathcal{U}}(t) \leq \varepsilon_{\mathcal{U}}, \\ & \qquad A_{eq}^{\mathcal{O}}\, \mathcal{X}_{\mathcal{O}}(t) = b_{eq}^{\mathcal{O}}(t), \\ & \qquad A_{ineq}^{\mathcal{O}}\, \mathcal{X}_{\mathcal{O}}(t) \leq b_{ineq}^{\mathcal{O}}(t), \end{aligned} \tag{12}$$

where $\hat{\mathcal{U}}(t)$ are the measured values of the input variables, $\hat{\mathcal{Y}}(t)$ are the measured values of the output variables, $\Pi_{\mathcal{Y}}$ and $\Pi_{\mathcal{U}}$ are matrices that select the input and output variables from vector $\mathcal{X}_{\mathcal{O}}$, $\mathbf{1}_{\mathcal{Y}}$ and $\mathbf{1}_{\mathcal{U}}$ are vectors of unitary entries of dimensions $H_{\mathcal{O}} \cdot n_y$ and $H_{\mathcal{O}} \cdot n_u$, respectively, and $\varepsilon_{\mathcal{Y}}$ and $\varepsilon_{\mathcal{U}}$ are auxiliary variables used to reformulate the minimization of the 1-norms $\|\Pi_{\mathcal{Y}}\, \mathcal{X}_{\mathcal{O}}(t) - \hat{\mathcal{Y}}\|_1$ and $\|\Pi_{\mathcal{U}}\, \mathcal{X}_{\mathcal{O}}(t) - \hat{\mathcal{U}}\|_1$ as an MILP problem [4]. Finally, additional equalities $A_{eq}^{\mathcal{O}}\, \mathcal{X}(t) = b_{eq}^{\mathcal{O}}(t)$, and inequalities $A_{ineq}^{\mathcal{O}}\, \mathcal{X}(t) \leq b_{ineq}^{\mathcal{O}}(t)$, are analogous to those commented in Section 2.2 for the OCP case.

For a detailed formulation, see [23, 18]. A discussion on different state-of-the-art approaches to the formulation of optimization-based SEPs and their suitability for the sewer network regulation problem can also be found in those references.

2.4 Receding Horizon Control with Moving Horizon Estimation Algorithm

Receding Horizon Control (RHC) is an RTC strategy aimed to take full advantage of model-based control techniques, real-time measurements and disturbance forecasts. To this end, after solving a finite-horizon optimal control problem, only the part of the sequence of control actions obtained as a solution corresponding to the first time step is applied to the system. After letting the system respond to this action for the corresponding time step, measurements are taken. Using these measurements (and, if available, new disturbance forecasts) a new OCP is formulated and solved to compute the control action for the next time step and the whole procedure is repeated again. Depending on the available measurements, the initial conditions for each of the subsequent OCPs can be directly obtained or must be estimated. In the latter case, before solving each OCP, a SEP is solved to reconstruct the full-state initial condition necessary to formulate the OCP. The technique consisting in solving a fixed-length finite horizon SEP at each time step based on the last available measurements is known as Moving Horizon Estimation (MHE) and is regarded as the state estimation counterpart of the RHC strategy.

In some cases, the time step used in the control model to provide sufficient accuracy might not be adequate to be used in the RHC strategy as described above. This fact might be due to additional time required to gather system measurements from a SCADA system and formulate and solve the SEPs and OCPs or due to limitations in the actuators. In any case, the RHC/MHE strategy can still be applied by updating and solving the SEPs and OCPs every few time steps instead of at every one. The number of time steps t_c elapsed between updating and solving two consecutive SEPs and OCPs is called the *control interval*.

Algorithm 1 details the whole RHC/MHE procedure in terms of the OCPs and SEPs described in the previous sections for an event of t_s time steps. Variables with a star upper index indicate that they are the solution of the corresponding optimization problem.

Algorithm 1: RHC-MHE Algorithm

Input : $\mathcal{X}_0(1) = \left(\hat{X}(0)^\top, \ldots, \hat{X}(-T+1)^\top\right)^\top = \mathbf{0}$

begin

Set $t := 1$

while $t \leq t_s$ **do**

Compute rainfall-runoff prediction $R_H(t) = \left(r(t+1)^\top, \ldots, r(t+H)^\top\right)^\top$

Compute $\mathcal{M}_3(t)$, $\mathcal{N}_3(t)$, $b_{eq}(t)$, $b_{ineq}(t)$, $\mathcal{M}_2^{\mathcal{O}}(t)$, $\mathcal{N}_2^{\mathcal{O}}(t)$, from $\mathcal{X}_0(t)$, $R_H(t)$

Solve OCP$(t) \rightarrow \mathcal{X}^*(t) = \left(X^*(t+H)^\top, \ldots, X^*(t+1)^\top\right)^\top$

Let the system evolve during time interval $(t, t+t_c)$ with gate PID set-points $G_{PID} = G^*(t)$

Read measurements through the SCADA system: $\hat{\mathcal{U}}(t)$, $\hat{\mathcal{Y}}(t)$

Solve SEP$(t+t_c) \rightarrow \mathcal{X}_{\mathcal{O}}^*(t+t_c) = \left(X_{\mathcal{O}}^*(t+t_c)^\top, \ldots, X_{\mathcal{O}}^*(t+t_c-H_{\mathcal{O}}+1)^\top\right)^\top$

Set $\mathcal{X}_0(t+t_c) := \left(X_{\mathcal{O}}^*(t+t_c)^\top, \ldots, X_{\mathcal{O}}^*(t+t_c-T+1)^\top\right)^\top$

Set $t := t + t_c$

end

end

Regarding closed-loop stability (in the Bounded-Input Bounded-Output sense, [28]), notice first that due to the constraints added to the actuator flows in the OCPs, the setpoints for local controllers are always bounded by their maximum operative values, given by their physical properties. Therefore, instability can only be a consequence of overtuning of the local controllers. However, in a sewer network, the actuators (gates, pumps, weirs) cannot add any flow to the network but only redirect it: the outflow from an actuator is always limited by its upstream inflow (volume in case of an actuator controlling a tank). Therefore, even if the local controllers are not suitably tuned, it is not possible that the closed-loop system unstabilizes since the actual flow will be limited by the inflow to the actuator (which is finite, since the total rain inflow is finite). A poorly calibrated model of the system or overtuned local PID controllers can only lead to poor performance results and increased flooding events but never to unstable behavior.

3 Receding Horizon Control with Moving Horizon Estimation Results

3.1 Case Study and Simulation Algorithm

To test the proposed RHC/MHE strategy, an implementation of a real network in the physically-based model sewer network simulator MOUSE [12] has been used as virtual reality. In addition to simulating the flows along the whole network by means of the complete de Saint-Venant model, MOUSE is also able to simulate local PID controllers at network actuators. The studied network, called the Riera Blanca sewer network, is located in the city of Barcelona. The company responsible for the network management, CLABSA (Clavegueram de Barcelona, S.A.), has provided the MOUSE implementation of the network used in this study including detailed geometry, materials and hydrological parameters (rainfall catchment area and slope, surface storage and infiltration capacity, and perviousness, among others), which were calibrated by using real measurement data. The company has also provided the data corresponding to the four real rain events used for calibration and simulation which are moderate to strong events (with a return period of about two years), which require proper management of the network to avoid flooding.

Using data generated by the physically-based simulator, the model described in [22] was implemented, calibrated and validated for the case-study sewer network. After a mild topological simplification consisting in only considering junctions with more than just a single inflow (also taking into account rain

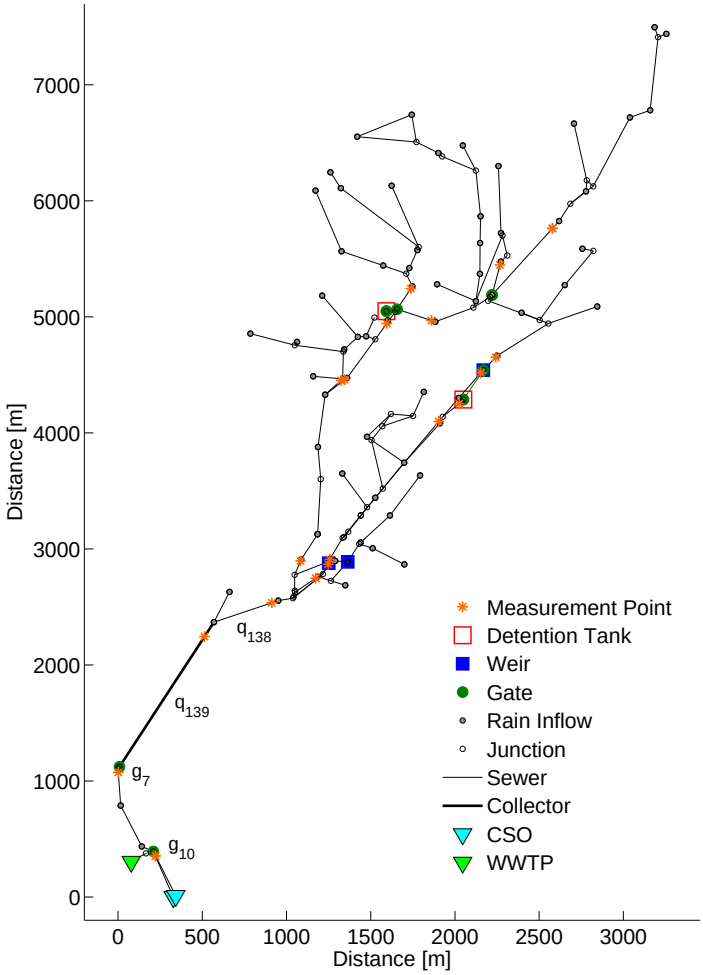

Figure 1: Riera Blanca sewer network after topological simplification and detail of its downstream part (adapted from [22]).

inflows) and a single outflow, the network consists of

$$
\begin{aligned}
n_v &= 2 \text{ tanks},\\
n_q &= 145 \text{ sewers},\\
n_w &= 3 \text{ weirs},\\
n_f &= 11 \text{ overflows},\\
n_g &= 10 \text{ gates},\\
n_c &= 1 \text{ collector},\\
n_r &= 68 \text{ rain inflows},\\
n_y &= 20 \text{ measurement points}.
\end{aligned}
$$

Figure 1 shows the network diagram after simplification. It can be noticed that the network converges at its downstream end to a collector (q_{139}) with a controlled gate at its downstream end (g_7). Collector q_{139} has a total volume of about 6.4×10^4 m^3, which can be used for in-line retention and is modeled using a tank equation with inflow delay, as detailed in [21]. All the flow released through gate g_7 is either routed to the WWTP or discharged to the Mediterranean sea as CSO. Since the WWTP has an inflow rate of just $2\,\mathrm{m}^3/\mathrm{s}$, the proper management of the storage capacity of collector q_{139} is of capital importance to minimize CSO discharges and maximize WWTP usage. Further details on the case study network can be found in [18, 22].

The management objectives for the Riera Blanca sewer network are:

1. Minimize overflows
2. Minimize CSO discharges

3. Maximize WWTP usage

These objectives are quantified in the following multi-objective cost function for the OCPs:

$$J(\mathcal{X}(t)) = \gamma_{COF}\, J_{COF}(\mathcal{X}(t)) + \gamma_{OF}\, J_{OF}(\mathcal{X}(t)) \; + \; \gamma_{CSO}\, J_{CSO}(\mathcal{X}(t)) - \gamma_{WWTP}\, J_{WWTP}(\mathcal{X}(t)), \tag{13}$$

where $J_{COF}(\mathcal{X}(t))$ is the overflow of collector q_{139}, $J_{OF}(\mathcal{X}(t))$ contains the sum of the rest of the overflow variables at junctions, $J_{CSO}(\mathcal{X}(t))$ contains the sum of flow variables corresponding to the sewers connecting the network to the sea and $J_{WWTP}(\mathcal{X}(t))$ contains the sum of flow variables corresponding to the sewers connecting the network to the WWTP. The values of the weights have been chosen as follows:

$$\begin{aligned} \gamma_{COF} &= 10, \\ \gamma_{OF} &= 1, \\ \gamma_{CSO} &= 1, \\ \gamma_{WWTP} &= 10^{-1}. \end{aligned}$$

A discussion on the choice of these values is provided in [22], together with some indications to determine them in an arbitrary network. As a result of the minimization of this objective function, flows through actuators are computed by the solver so that the undesired flows (overflow and CSO) are minimized and the desired ones (WWTP) maximized. This is achieved by using the gates to route part of the flow to the two detention tanks at the upper part of the network (see Figure 1) and by using gate g_7 to activate the storage capacity of sewer q_{139} to retain the incoming volume while providing an outflow that can be handled by the WWTP whenever possible.

In the Riera Blanca sewer network, to provide a suitable approximation of the flow delay in the sewers, a sampling time of $\Delta t = 1$ minute was chosen. Taking into account that gates can only be moved at limited speeds, this time step is not sufficient for the local controllers to achieve the gate flow set-points $G^*(t)$ obtained as the solution of the OCPs. Therefore, a control interval of $t_c = 5$ time steps (i.e., five minutes) was chosen and the set-points produced by the OCP are assumed to be constant for five minutes periods. To take this into account in the control model, a constraint forcing gate flows to remain constant along five time steps was added to the OCPs.

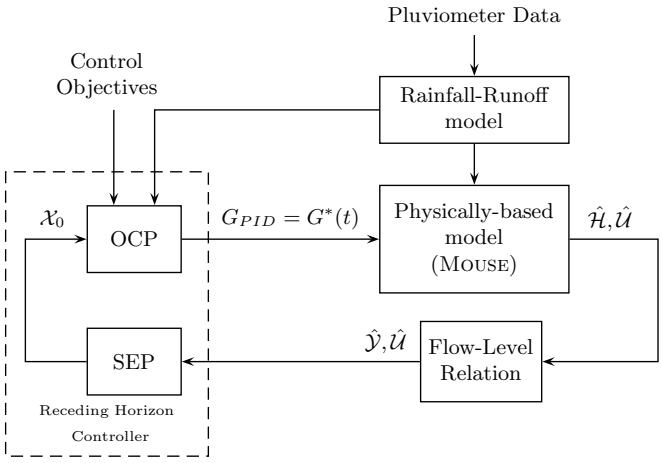

Figure 2: Closed-loop simulation algorithm diagram with water level measurements, denoted by $\hat{\mathcal{H}}$ (adapted from [22]).

By performing simulations with MOUSE, the SCADA measurements mentioned in Algorithm 1 can be substituted by the results of the simulations. Since these results provide complete information of all the flows and water levels in the network, by selecting the variables to be used when solving the SEPs, different measurement availability scenarios can be tested.

According to Algorithm 1, at time instant t an SEP with an estimation horizon of $H_o = 15$ time steps is solved. The solution values corresponding to the last $T = 6$ time steps are used as initial conditions to formulate and solve an OCP with a prediction horizon $H = 40$ time steps. The (constant) values of the gate flows for the first five minutes are used as set-points for PID controllers implemented in MOUSE to run a simulation of the system evolution during five minutes. The result of this simulation is then

used to obtain the system measurements to formulate and solve the SEP at time instant $t + 5$ and the procedure is repeated again. Figure 2 shows a diagram of this procedure. Notice that, since the model, and therefore the OCPs, are based only on both flow and volume variables, water level measurements must be transformed into flow ones by means of some flow-level relation before solving the SEPs, as described in Section 3.4.

3.2 Simulation Algorithm Implementation

According to the RHC/MHE strategy described above, for the simulation of a closed-loop control event a series of SEPs, OCPs and physically-based model simulations (substituting the real evolution of the system) must be solved and executed.

From an implementation point of view, closed-loop simulations require a bidirectional communication between the physically-based simulator and the optimization module. The overall closed-loop simulation algorithm is written as a MATLAB script, which calls the numerical solver for the SEPs and OCPs and calls the simulator executable through command line orders.

The results of the OCPs and SEPs are directly obtained as MATLAB vectors and no post-processing is required. The elements of the OCP solution vector corresponding to the gate flow set-points are written in the simulator configuration files by the MATLAB script before running the simulations. The result of these simulations are binary files that must be extracted into text files, again using command line orders called by the MATLAB script. Finally, the text files are read by the MATLAB script and transformed into the "measurement data" vectors needed to formulate the next SEP and OCP.

3.3 State-Feedback RHC Results

The first test to assess the performance of the proposed RHC strategy is carried out assuming a rather improbable situation in which measurements of the network flows are available at all the network sewers, gates and weirs. In this case, in Algorithm 1, no SEP needs to be solved, since, using the measured flows, the rest of the model variables can be computed through the model equations. Although assuming full-flow measurement is unrealistic, the results of this test will be useful as a reference to assess the performance of the RHC strategy when used together with the MHE technique. From now on, this measurement scenario will be referred to as Full-State Measurement (FSM).

Table 1: RHC with FSM results and variations with respect to passive control.

Episode	Overflow [$\times 10^3 m^3$]	CSO [$\times 10^3 m^3$]	WWTP [$\times 10^3 m^3$]
17-09-2002	0.16 (-96.26%)	9.21 (-91.04%)	107.20 (75.57%)
09-10-2002	1.01 (-96.09%)	341.74 (-31.56%)	101.27 (20.38%)
15-08-2006	0.25 (-96.40%)	4.87 (-94.60%)	100.71 (117.20%)
30-07-2011	0.75 (-95.95%)	39.38 (-72.85%)	108.14 (125.48%)

Table 1 shows the results obtained from those simulations and the variations in the objectives compared with the results obtained by simulating the rain events with gates set at fixed positions (*passive control*). The actual network regulation is performed by expert operators and no data related to the real management of the network for the considered rain scenarios is available for comparison. Results show that an appropriate management of the detention tanks at the upper part of the network can mitigate overflows almost completely by reducing the peak flows in the network sewers (most overflow volume reported in Table 1 corresponds to overflow points upstream of any control action). The volume stored into the tanks can be released later at adequate flow rates to maximize the use of the WWTP capacity. On the other hand, the proper use of the detention tanks and the in-line storage capacity of sewer q_{139} yields a considerable reduction of the CSO volumes.

3.4 Output-Feedback RHC/MHE Results

Due to the large-scale nature of sewer networks, the most common situation is that measurements of the network variables are only available at certain points. Moreover, instrumentation for water level measurements is cheaper, more reliable and requires less maintenance than that aimed to measure flow rates (for details on instrumentation for level and flow measurements in sewer networks see [5, 38]). To take

into account these facts, the model-based RHC/MHE strategy proposed in this paper has been applied to the case study network taking into account the available instrumentation. In fact, only level measurements through limnimeters are available in the Riera Blanca network. The measurement points are depicted with stars in Figure 1. Since the local PID controllers at the gates implemented in the physically-based model simulator use flow measurements to regulate the gate position, it has been assumed in the following that flow measurements are always available at the gate outputs. Notice that flow-level relations near gates (in general, near hydraulic structures) are well known and described in a number of classic open channel flow references [7, 16]. These relations allow to obtain accurate flow approximations from level measurements. In fact, the physically-based model used in this work as virtual reality makes use of these formulas to impose internal conditions among sewers connected by gates [10]. Therefore, instead of re-implementing the formulas described in the software documentation, flow values are directly used. If, by means of a measurement, the level at a gate outflow is found to be below the gate leaf, the gate relations mentioned above should be replaced by other approximated flow-level relation such as the polynomials used in other points of the network.

In the following, the performance of the model according to four configurations regarding the available measurements are compared and discussed:

- Flow measurements at the limnimeter locations (from now on, this scenario will be referred to as MHEF)
- Water level measurements at the limnimeter locations (from now on, this scenario will be referred to as MHEL)
- Water level measurements at the limnimeter locations plus flow measurement at the collector inflow (from now on, this scenario will be referred to as MHEC)
- Water level measurements at the limnimeter locations plus flow measurement at the collector inflow and at the collector's upstream sewer inflow (from now on, this scenario will be referred to as MHEC2)

3.4.1 Flow-Level Relation

Notice that, since the model does not contain water levels but flows, in the last three scenarios, water level measurements must be converted to flow values. To compute flow values from water level measurements, third-degree polynomial approximations for the flow-level relation have been used, i.e.,

$$\hat{q}(t) = p_0\,\hat{h}(t)^3 + p_1\,\hat{h}(t)^2 + p_2\,\hat{h}(t) + p_3, \tag{14}$$

where $\hat{h}(t)$ is the measured water level and $\hat{q}(t)$ the flow approximation (the symbol $\hat{}$ is used in the following to denote values obtained from measurements/simulations, as opposite to those generated by the control model). Calibration of the polynomial coefficients $p_i,\ i = 0,\ 1,\ 2,\ 3$, has been performed by means of least squares fitting using data from four rain events. The resulting coefficients for each rain event have been averaged to obtain the final set of coefficients. The choice of the polynomial degree is based on trial and error tests, which showed that no improvement in the fitting is obtained using higher degrees.

Once the flow variables have been recovered by using the flow-level approximations, the SEP and OCP are solved as in the flow measurements case, as shown in Figure 2.

Polynomial approximations for flow-level relations are accurate when they are applied to sewers that are not affected by backwater effects. However, for collector q_{139}, the presence of the downstream gate causes the flow-level relation to become not even one to one. This effect is even increased if the gate position changes: the loop shape present in the flow-level relation for calibration data with a fixed downstream gate becomes a much more complex curve in the case of a moving gate leading to poor polynomial approximations, as shown in Figure 3.

3.4.2 SEP Results

To assess the performance of the state estimation strategy in approximating the initial conditions for the OCPs, two error indices have been defined. First, for each sewer $i = 1, \ldots, n_q$, and each SEP solved

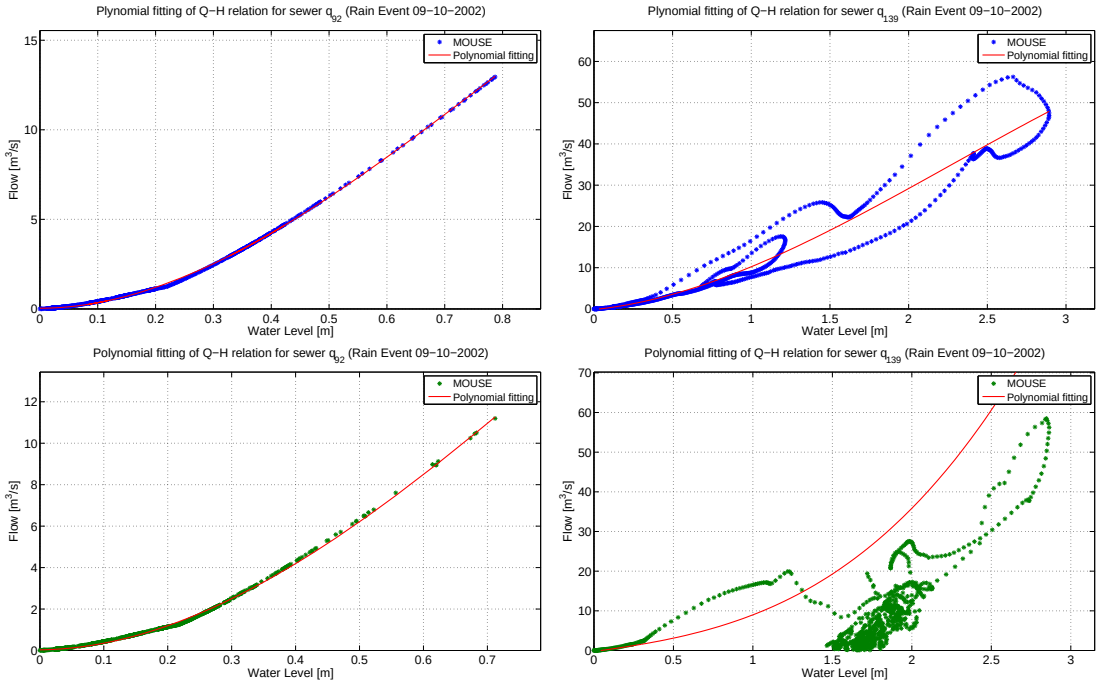

Figure 3: Polynomial approximation of the flow-level relations for a free-flow upstream sewer (q_{92}) and a backwater-affected downstream one (q_{139}) corresponding to the rain event 09-10-2002 with fixed gate positions (blue) and for the MHEL closed-loop simulation scenario (green). The polynomial coefficients correspond to a single event fitting.

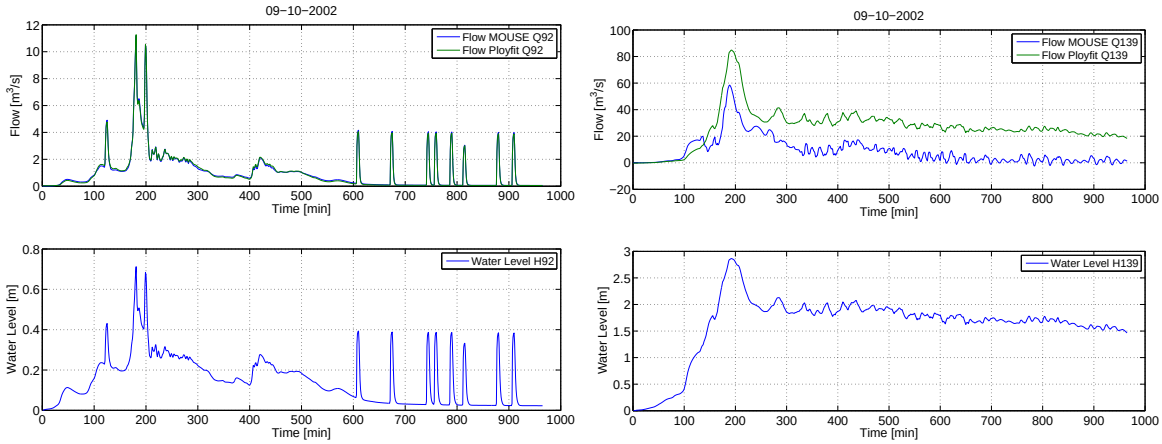

Figure 4: Polynomial flow-level estimation for a free-flow upstream sewer (q_{92}) and a backwater-affected downstream one (q_{139}) for the MHEL closed-loop simulation scenario and rain scenario 09-10-2002.

$k = 1, \ldots, t_s/5$, the maximum error in the last T estimates (that is, the values used in the OCP updating) is computed as

$$e_i^{\mathcal{O}}(k) = \max_{\tau=5\,k-T+1,\ldots,5\,k} |\hat{q}_i(\tau) - q_i^{\mathcal{O}}(\tau)| \quad \left[\frac{\mathrm{m}^3}{\mathrm{s}}\right]. \tag{15}$$

And secondly, the previously defined maximum error is averaged over all the solved SEPs, i.e.,

$$\bar{e}_i^{\mathcal{O}} = \frac{5}{t_s} \sum_{k=1}^{t_s/5} e_i^{\mathcal{O}}(k) \quad \left[\frac{\mathrm{m}^3}{\mathrm{s}}\right]. \tag{16}$$

These error indices provide a measure for the state estimation accuracy for each network sewer. Finally, to obtain a description of the overall performance of the state estimation for the whole network, define

$$E_{\mathcal{O}} = \left(\bar{e}_1^{\mathcal{O}}, \bar{e}_2^{\mathcal{O}}, \ldots, \bar{e}_{n_q-1}^{\mathcal{O}}, \bar{e}_{n_q}^{\mathcal{O}}\right). \tag{17}$$

Table 2 provides the mean, maximum and variance values of vector $E_{\mathcal{O}}$. The maximum error values always occur for the estimation of the flow at the collector q_{139} and its immediate upstream sewer q_{138}. These errors are mainly caused by the presence of backwater effects and by the fact that those sewers show the highest flow values and variation rates as a consequence of being at the downstream end of the network, where all flows converge. In Figure 5, plots of the flows obtained as the solution of several consecutive SEPs (including the one with the highest maximum error) and the corresponding flow values to be estimated are shown for collector q_{139} (for the MHEL scenario the flow obtained from the polynomial flow-level transformation is also shown).

It can be noticed from Table 2 and Figure 5 that when flow measurements are used (MHEF scenario), the flow estimates provided by the SEP, thanks to the hydraulic model, are quite close to the values provided by the physically-based model simulator. On the other hand, for the water level measurements scenario MHEL, the collector inflow is considerably overestimated. This is because the solution of the SEPs aims to produce flows close to the ones obtained from the flow-level relation, rather than the actual flows, which, as discussed in Section 3.4.1, are not accurate in case of backwater effects. By adding a flow measurement at the collector inflow (MHEC scenario), estimates of the collector flow are partially corrected, but still suffer from the influence of the flow-level approximation at the sewer upstream of the collector, which is also affected by backwater. Finally, measuring flows at both the collector and its upstream sewer, the obtained results become closer to those obtained with the MHEF scenario, since flow-level transformations in upstream sewers produce suitable approximations. Taking into account that flows at the collector reach values of 30 to 50 m^3/s, the average maximum error between 2 and 4 m^3/s of the MHEF, MHEC and MHEC2 scenarios (Figure 5) means that the approximations are sufficiently accurate to be used in a RHC scheme. For the MHEL case, however, the high errors in the collector inflow estimation lead to a considerable performance loss, as discussed in the next section.

3.4.3 Closed-Loop RHC/MHE Results

Table 3 collects the performance results for the four RHC/MHE scenarios and the RHC with full-state measurement (FSM) ones according to the three management objectives defined in Section 3.1. It can be noticed that a minimal variation of the overflow and WWTP objectives is obtained with the different measurement approaches. Overflows occur in the upper to middle part of the network and are avoided by redirecting part of the flow to the detention tanks. The presence of measurements at the sewers upstream of the gates redirecting flow to the tanks and the accurate approximations by means of the flow-level relation at those locations guarantee a proper management of the tanks and an optimal mitigation of overflows. Regarding the WWTP objective, results are quite similar in all measurement scenarios since in all cases the plant receives its maximum inflow all the time since soon after the beginning of the rain event.

The most noticeable variations that can be observed in Table 3 are regarding the CSO values. The fulfillment of this objective is closely related to the proper use of the in-line retention capacity of the collector, which is in turn related to the accuracy of the flow approximations at its inflow and at its upstream sewer inflow. The performance results for the CSO objective are, therefore, correlated with the accuracy of the SEPs in estimating the collector inflow. Accordingly, it can be noticed from Table 3 that the CSO volume corresponding to the MHEF scenario is very close to that obtained in the FSM one. On the other hand the MHEL scenario provides the highest CSO volumes, since the overestimation of the

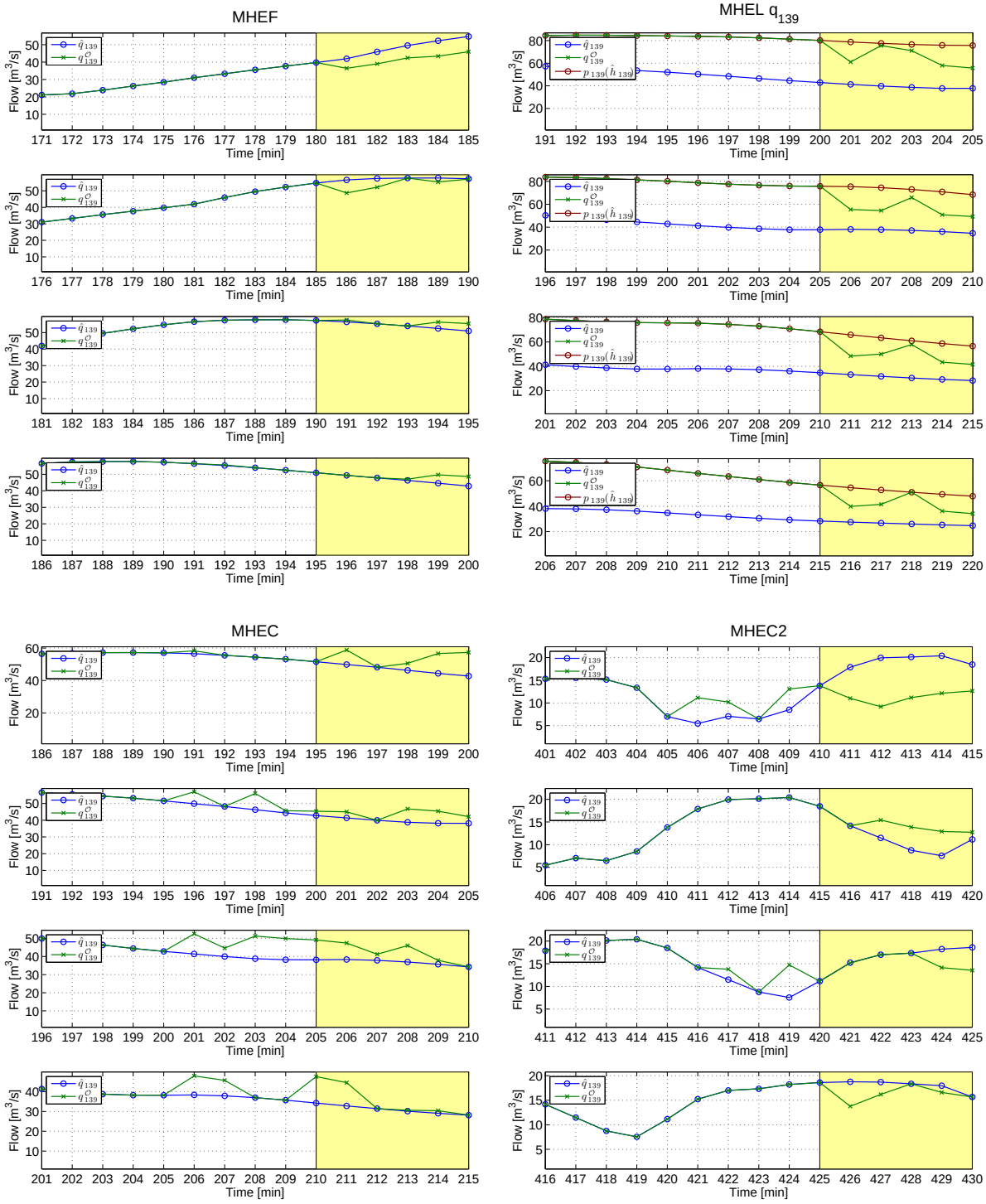

Figure 5: SEP solutions of several consecutive problems for collector q_{139} corresponding to the different measurement scenarios (rain event 09-10-2002). The first plot of each measurement scenario corresponds to the maximum absolute error $\bar{e}^{\mathcal{O}}_{139}$ obtained among all the solved SEPs.

Table 2: Mean, maximum and variance of the averaged maximum error $E_{\mathcal{O}}$.

Episode	Measurement Scenario	Mean($E_{\mathcal{O}}$) [m^3/s]	Max($E_{\mathcal{O}}$) [m^3/s]	Var($E_{\mathcal{O}}$) [m^3/s]
17-09-2002	MHEF	0.12	1.50	0.03
	MHEL	0.26	10.91	1.09
	MHEC	0.18	2.98	0.15
	MHEC2	0.12	1.50	0.03
09-10-2002	MHEF	0.13	1.57	0.04
	MHEL	0.34	12.93	1.48
	MHEC	0.24	3.65	0.21
	MHEC2	0.18	2.15	0.07
15-08-2006	MHEF	0.09	1.18	0.02
	MHEL	0.19	7.34	0.49
	MHEC	0.13	1.66	0.06
	MHEC2	0.09	1.16	0.02
30-07-2011	MHEF	0.11	1.87	0.04
	MHEL	0.29	12.34	1.39
	MHEC	0.20	3.27	0.19
	MHEC2	0.12	1.73	0.04

Table 3: RHE/MHE results and comparison with state feedback (FSM, Table 1).

Episode	Measurement Scenario	Overflow [$\times 10^3 m^3$]	CSO [$\times 10^3 m^3$]	WWTP [$\times 10^3 m^3$]
17-09-2002	FSM	0.16	9.21	107.20
	MHEF	0.16 (0.00%)	4.06 (-55.86%)	107.43 (0.21%)
	MHEL	0.16 (0.00%)	32.61 (254.16%)	106.06 (-1.07%)
	MHEC	0.16 (0.00%)	17.06 (85.30%)	106.02 (-1.11%)
	MHEC2	0.16 (0.00%)	3.78 (-58.95%)	106.46 (-0.69%)
09-10-2002	FSM	1.01	341.74	101.27
	MHEF	1.08 (7.52%)	340.90 (-0.24%)	101.56 (0.28%)
	MHEL	1.01 (0.48%)	364.10 (6.55%)	100.81 (-0.45%)
	MHEC	1.03 (2.26%)	354.83 (3.83%)	100.90 (-0.37%)
	MHEC2	1.01 (0.02%)	333.63 (-2.37%)	101.12 (-0.15%)
15-08-2006	FSM	0.25	4.87	100.71
	MHEF	0.25 (0.00%)	5.26 (8.21%)	100.61 (-0.10%)
	MHEL	0.25 (0.00%)	11.04 (127.01%)	99.57 (-1.13%)
	MHEC	0.25 (0.00%)	6.16 (26.71%)	99.58 (-1.12%)
	MHEC2	0.25 (0.00%)	5.74 (17.93%)	99.91 (-0.79%)
30-07-2011	FSM	0.75	39.38	108.14
	MHEF	0.75 (0.00%)	41.55 (5.51%)	108.18 (0.04%)
	MHEL	0.75 (0.00%)	67.49 (71.38%)	107.27 (-0.80%)
	MHEC	0.75 (0.00%)	56.36 (43.11%)	107.14 (-0.93%)
	MHEC2	0.75 (0.00%)	40.13 (1.90%)	107.56 (-0.54%)

collector inflow leads also to an overestimation of the collector volume, causing its in-line storage capacity not to be fully used. By adding a single flow measurement at the collector inflow (MHEC scenario), the CSO volume is slightly reduced with respect to the MHEL case, but the influence of the flow-level approximations at the collector upstream sewer q_{138} still has a negative effect. Finally, by adding a second flow measurement at sewer q_{138}, the MHEC2 scenario provides results similar to those with flow

measurements in the MHEF and the FSM scenarios. Therefore, it can be concluded that by installing of two flow-meters at the collector inflow and upstream sewer, the CSO volume could be considerably reduced.

3.5 Computational Details

All optimization problems were solved using CPLEX v12.5 [8] MILP solver with standard settings, available thanks to IBM Academic Initiative [17], on a desktop with an Intel Core 2 Duo CPU with 3.33 GHz and 8 GB RAM and on a laptop with an Intel Core i7 CPU with 2.2 GHz and 8 GB RAM.

Tables 4 and 5 show respectively the size and computational times needed to solve the OCP and SEP for the different measurement scenarios and rain events. It is a very important feature of the whole modeling and control approach that these problems can be solved within short times so that the whole real-time RHC strategy can be implemented. It can be noticed that almost all the maximum times needed to solve the OCPs are below 10 seconds, with a single maximum instance of 22 seconds, which are suitable times for a real-time controller taking into account that the control interval is of five minutes.

Table 4: Details on the number of variables and constraints of the OCPs and SEPs.

	OCP	SEP
Continuous variables	8520	3645
Discrete variables	1040	390
Equality constraints	7440	1783
Inequality constraints	7240	2510

Table 5: OCP and SEP computational details for the different measurement scenarios and rain events.

Episode	Measurement Scenario	OCP		SEP			
		Mean Time [s]	Max Time [s]	Mean Time [s]	Max Time [s]	Max RMIPG	Time Limit Violations
17-09-2002	FSM	0.59	1.61	-	-	-	-
	MHEF	0.42	1.25	3.36	60.12	0.68 %	2
	MHEL	0.43	1.39	3.76	60.05	0.47 %	3
	MHEC	0.42	0.92	3.48	60.03	0.31 %	1
	MHEC2	0.43	0.94	3.27	60.17	0.38 %	2
09-10-2002	FSM	0.65	1.70	-	-	-	-
	MHEF	0.62	3.23	4.44	60.03	0.75 %	3
	MHEL	0.60	5.41	6.92	60.05	0.92 %	6
	MHEC	0.67	21.98	5.13	60.03	0.76 %	4
	MHEC2	0.61	5.41	5.01	60.05	0.32 %	3
15-08-2006	FSM	0.59	2.20	-	-	-	-
	MHEF	0.49	3.33	2.81	36.47	0.01 %	0
	MHEL	0.44	3.20	2.71	42.72	0.01 %	0
	MHEC	0.42	2.58	3.07	60.05	0.08 %	1
	MHEC2	0.41	1.69	2.92	60.03	0.02 %	1
30-07-2011	FSM	0.58	1.67	-	-	-	-
	MHEF	0.45	2.20	3.03	51.25	0.01 %	0
	MHEL	0.44	2.14	3.46	60.03	0.09 %	2
	MHEC	0.44	1.61	2.81	60.03	0.12 %	1
	MHEC2	0.47	1.84	2.57	60.02	0.02 %	1

On the other hand, the SEPs have been proven harder to solve. Even though they have less than half the number of variables than the OCPs (c.f. Table 4), longer computational times are needed to reach the

optimal solution due to stronger conflict among the individual objectives in the cost function (a proper fitting at a particular measurement point can cause a poorer one at another point), which requires a higher number of iterations before optimality can be guaranteed. To ensure the computational times within each RHC/MHE iteration to be suitable for a RTC application, a time limit of 1 minute has been set for all the SEPs, provided a feasible suboptimal solution is available. Therefore, when the maximum SEP time shown in Table 5 is above 60 seconds, it means that the optimization has been stopped due to violation of the time limit constraint and that the best feasible solution found so far has been used to continue with the RHC/MHE iterations. The last two columns in Table 5 show the maximum percentage of suboptimality of the best feasible solution found in the SEPs for which the optimization has prematurely stopped due to the time limit constraint and the number of times this situation has occurred out of 193 SEP instances solved for each rain event.

According to the CPLEX documentation [8], the suboptimality index, called the *Relative MIP Gap* (RMIPG), provides an upper bound on the relative difference between the best feasible solution found by the solver by the time the optimization is terminated and the optimal solution. It is computed taking into account the solutions of intermediate subproblems solved during the branching algorithm used to solve, in turn, the corresponding MILP problems.

The number of violations of the time constraint and their corresponding values of the RMIPG (as a percentage) in Table 5 show that the situation is not common, and even in those cases the obtained suboptimal solution is sufficiently close to the optimal one to be used without problems in the RHC/MHE iterations. Notice that when the time constraint is not violated, the RMIPG value is always 0.01%, since this is the default value below which the solver considers that the best integer solution is already the optimal one and the algorithm terminates.

4 Conclusions and Future Work

Receding Horizon Control is widely regarded as one of the best options for the regulation of combined sewer networks since it can take advantage of model-based predictions of the network state using instantaneous measurements and rainfall forecasts. However, in real applications on large-scale sewer networks only a limited number of measurements are usually available, difficulting the implementation of Receding Horizon Controllers, which require full-state knowledge to formulate Optimal Control Problems. In this paper, the problem of estimating the state vector of a sewer network from a few measurements to perform model-based Optimal Control in a Receding Horizon Control strategy has been addressed.

The proposed model-based State Estimation Problems, iteratively solved in a Moving Horizon Estimation strategy, have proven to produce accurate estimates of the network flows, provided accurate flow measurements or approximations are available. Unfortunately, it has also been shown that flow-level relations in sewers affected by backwater effects result in poor flow approximations that, in turn, have a negative effect over both the accuracy of the state estimates and the overall RHC/MHE performance. This problem may be overcome by adding a limited number of flow sensors to improve the state estimation at these specific locations. In the context of this paper, by adding two flow sensors in the case study, the performance of the proposed control methodology and simulation algorithm have been shown to be comparable to what could be expected if full knowledge of the states was available.

To further develop the proposed RHC/MHE strategy, improved approximations of the flow-level relations in presence of backwater are being developed to take advantage of additional water level measurements along the same collector as well as measurements of the downstream gate position.

Acknowledgements

This work has been partially funded by the research project ECOCIS (DPI–2013–48243–C2–1–R). Data to support this article is property of CLABSA and is not available to public access due to privacy policies. The authors are especially grateful for the collaboration of the CLABSA staff in providing the test case, data and expert guidance.

References

[1] Bemporad, A., Ferrari-Trecate, G., and Morari, M. Observability and controllability of

piecewise affine and hybrid systems. *IEEE Transactions on Automatic Control 45*, 10 (2000), 1864–1876.

[2] Bemporad, A., Mignone, D., and Morari, M. Moving horizon estimation for hybrid systems and fault detection. In *Proceedings of the American Control Conference* (San Diego, USA, 1999), pp. 2471–2475.

[3] Bemporad, A., and Morari, M. Control of systems integrating logic, dynamics, and constraints. *Automatica 35*, 3 (1999), 407–427.

[4] Boyd, S., and Vandenberghe, L. *Convex Optimization*. Cambridge University Press, Cambridge, 2004.

[5] Campisano, A., Cabot Ple, J., Muschalla, D., Pleau, M., and Vanrolleghem, P. Potential and limitations of modern equipment for real time control of urban wastewater systems. *Urban Water Journal 10*, 5 (2013), 300–311.

[6] Cembrano, G., Quevedo, J., Salamero, M., Puig, V., Figueras, J., and Martí, J. Optimal control of urban drainage systems. A case study. *Control Engineering Practice 12*, 1 (2004), 1–9.

[7] Chow, V. T. *Open-Channel Hydraulics*. McGraw-Hill, New York, 1959.

[8] CPLEX™. *version 12.5 (2012)*. IBM ILOG, Sunnyvale, California, 2011.

[9] Darsono, S., and Labadie, J. Neural-optimal control algorithm for real-time regulation of in-line storage in combined sewer systems. *Environmental Modelling & Software 22* (2007), 1349–1361.

[10] DHI Software. *MOUSE Pipe Flow – Reference Manual*. DHI Water & Environment, 2007.

[11] DHI Software. *MOUSE Surface Runoff Models – Reference Manua*. DHI Water & Environment, 2007.

[12] DHI Software. *MOUSE User Guide*. DHI Water & Environment, 2007.

[13] Duchesne, S., Mailhot, A., and Villeneuve, J.-P. Predictive real time control of surcharged interceptors: impact of several control parameters. *Journal of the American Water Resources Association 39*, 1 (2003), 125–135.

[14] Ferrari-Trecate, G., Mignone, D., and Morari, M. Moving horizon estimation for hybrid systems. *IEEE Transactions on Automatic Control 47*, 10 (2002), 1663–1676.

[15] Gelormino, M., and Ricker, N. Model-predictive control of a combined sewer system. *International Journal of Control 59*, 3 (1994), 793–816.

[16] Henderson, F. M. *Open channel flow*. Macmillan, 1966.

[17] IBM ILOG. IBM Academic Initiative. `http://www.ibm.com/academicinitiative`, 2013.

[18] Joseph-Duran, B. *Hybrid Modelling and Receding Horizon Control of Combined Sewer Networks*. PhD thesis, Universitat Politècnica de Catalunya, Automatic Control Department, Barcelona, Spain., 2014.

[19] Joseph-Duran, B., Jung, M., Ocampo-Martinez, C., Sager, S., and Cembrano, G. Minimization of sewage network overflow. *Water Resources Management 28*, 1 (2014), 41–63.

[20] Joseph-Duran, B., Ocampo-Martinez, C., and Cembrano, G. Receding horizon control of hybrid linear delayed systems: Application to sewer networks. In *Proceedings of the 52nd IEEE Conference on Decision and Control* (Firenze, Italy, 2013), pp. 2257–2262.

[21] Joseph-Duran, B., Ocampo-Martinez, C., and Cembrano, G. Hybrid control-oriented modeling of combined sewer networks: Barcelona case study. *Hydroinformatics Conference* (2014). New York, USA.

[22] Joseph-Duran, B., Ocampo-Martinez, C., and Cembrano, G. Hybrid modeling and receding horizon control of sewer networks. *Water Resources Research 50*, 11 (2014), 8497–8514.

[23] Joseph-Duran, B., Ocampo-Martinez, C., and Cembrano, G. Output-feedback control of sewer networks through moving horizon estimation. In *Proceedings of the 53rd IEEE Conference on Decision and Control* (Los Angeles, USA, 2014), pp. 1061–1066.

[24] Marinaki, M., and Papageorgiou, M. *Optimal Real-time Control of Sewer Networks*. Springer, London, 2005.

[25] Michalska, H., and Mayne, D. Moving horizon observers and observer based control. *IEEE Transactions on Automatic Control 40*, 6 (1995), 995–1006.

[26] Ocampo-Martínez, C. *Model predictive control of wastewater systems*. Advances in industrial control. Springer, London, 2011.

[27] Ocampo-Martínez, C., Puig, V., Cembrano, G., and Quevedo, J. Application of predictive control strategies to the management of complex networks in the urban water cycle [applications of control]. *IEEE Control Systems 33*, 1 (2013), 15–41.

[28] Proakis, J., and Manolakis, D. *Digital Signal Pocessing. Principles, Algorithms and Applications*, 4th ed. No. number. Prentice Hall, New Jersey, 2007.

[29] Puig, V., Cembrano, G., Romera, J., Quevedo, J., Aznar, B., Ramón, G., and Cabot, J. Predictive optimal control of sewer networks using CORAL tool: application to Riera Blanca catchment in Barcelona. *Water Science and Technology 60*, 4 (2009), 869–878.

[30] Rao, C., Rawlings, J., and Lee, J. Constrained linear state estimation–a moving horizon approach. *Automatica 37* (2001), 1619–1628.

[31] Rao, C., Rawlings, J., and Mayne, D. Constrained state estimation for nonlinear discrete-time systems: stability and moving horizon approximations. *IEEE Transactions on Automatic Control 48*, 2 (2003), 246–258.

[32] Rauch, W., Bertrand-Krajewski, J.-L., Krebs, P., Mark, O., Schilling, W., Schütze, M., and Vanrolleghem, P. Mathematical modelling of integrated urban drainage systems. *Water Science and Technology 45*, 3 (2002), 81–94.

[33] Rawlings, J., and Mayne, D. *Model Predictive Control: Theory and Design*. Nob Hill Publishing, Madison, 2009.

[34] Sadowska, A., De Schutter, B., and van Overloop, P.-J. Delivery-oriented hierarchical predictive control of an irrigation canal: event-driven versus time-driven approaches. *IEEE Transactions on Control Systems Technology* (2015). DOI: 10.1109/TCST.2014.2381600.

[35] Schütze, M., Butler, D., and Beck, M. *Modelling, Simulation and Control of Urban Wastewater Systems*. Springer, London, 2002.

[36] Schwanenberg, D., Verhoeven, G., and Raso, L. Nonlinear model predictive control of water resources systems in operational flood forecasting. *55th Internationales Wessenchaftliches Kolloquium* (2010).

[37] Schütze, M., Campisano, A., Colas, H., Schilling, W., and Vanrolleghem, P. Real time control of urban wastewater systems - where do we stand today? *Journal of Hydrology 299*, 3–4 (2004), 335–348.

[38] USEPA. Real Time Control of Urban Drainage Networks. U.S. Environmental Protection Agency Report 600-R-06-120, 2006.

[39] Vezzaro, L., and Grum, M. A generalised dynamic overflow risk assessment (DORA) for real time control of urban drainage systems. *Journal of Hydrology 515* (2014), 292 – 303.

[40] Xu, M., Negenborn, R., van Overloop, P., and van de Giesen, N. De Saint-Venant equations-based model assessment in model predictive control of open channel flow. *Advances in Water Resources 49* (2012), 37–45.